Separation Science and Technology

ISSN: 0149-6395 (Print) 1520-5754 (Online) Journal homepage: http://www.tandfonline.com/loi/lsst20

Pirimicarb degradation by $BiVO_4$ photocatalysis: Parameter and reaction pathway investigations

Yushen Wu, Chiingchang Chen, Yanchi Huang, Weiyu Lin, Yunting Yen & Chungshin Lu

To cite this article: Yushen Wu, Chiingchang Chen, Yanchi Huang, Weiyu Lin, Yunting Yen & Chungshin Lu (2016) Pirimicarb degradation by $BiVO_4$ photocatalysis: Parameter and reaction pathway investigations, Separation Science and Technology, 51:13, 2284-2296, DOI: 10.1080/01496395.2016.1202279

To link to this article: http://dx.doi.org/10.1080/01496395.2016.1202279

Accepted author version posted online: 21 Jun 2016.
Published online: 21 Jun 2016.

SEPARATION SCIENCE AND TECHNOLOGY
2016, VOL. 51, NO. 13, 2284–2296
http://dx.doi.org/10.1080/01496395.2016.1202279

Taylor & Francis
Taylor & Francis Group

Pirimicarb degradation by $BiVO_4$ photocatalysis: Parameter and reaction pathway investigations

Yushen Wu[a], Chiingchang Chen[b], Yanchi Huang[a], Weiyu Lin[a], Yunting Yen[c], and Chungshin Lu[d]

[a]Department of Environmental Engineering, HungKuang University, Sha-Lu, Taichung, Taiwan, Republic of China; [b]Department of Science Application and Dissemination, National Taichung University of Education, Taichung, Taiwan, Republic of China; [c]Department of Chemistry, Chung Yuan Christian University, Chung-Li, Taiwan, Republic of China; [d]Department of General Education, National Taichung University of Science and Technology, Taichung, Taiwan, Republic of China

ABSTRACT

In this study, bismuth vanadate is used as a visible-light catalyst for the photocatalytic degradation of pirimicarb insecticide. Significant amount of H_2O_2 is mandatory to obtain a significant photocatalytic activity of $BiVO_4$. The scavenger study indicates that holes and hydroxyl radicals are the main active species involved in the degradation of pirimicarb. Seven intermediates are identified and characterized through a mass spectra analysis. Based on this intermediate identification, a simple degradation pathway is proposed for the pirimicarb molecule, mainly through dealkylation and decarbamoylation. The practicality of this $BiVO_4$ photocatalyst is validated for the degradation of pirimicarb in environmental water samples, which indicates its potential for practical applications in water pollutant removal and environmental remediation.

ARTICLE HISTORY
Received 31 December 2015
Accepted 13 June 2016

KEYWORDS
Bismuth vanadate; degradation pathway; intermediate; pirimicarb

Introduction

Pirimicarb (2-dimethylamino-5,6-dimethylpyrimidin-4-yldimethylcarbamate) is an important substituted *N*-dimethylcarbamate insecticide and has been widely used against aphids in fruits and vegetables.[1,2] It is a suspected carcinogen and mutagen, and is acutely toxic for mammals due to its inhibition of the enzyme acetylcholinesterase.[3–5] Soloneski and Larramendy[6] have revealed that pirimicarb exerts both genotoxicity and cytotoxicity in Chinese hamster ovary (CHO-K1) cells. Pirimicarb has been classified as moderately hazardous (class II) by the World Health Organization (WHO).[7] Due to its extensive usage, pirimicarb has been detected frequently in environmental waters,[8,9] raising the need for the development of a simple and effective removal method.

Traditional wastewater treatment techniques include activated carbon adsorption, chemical oxidation, biological treatments, etc. However, each has limitations and disadvantages. The adsorption method involves only a phase transfer of pollutants without degradation, the chemical oxidation method is unable to mineralize all organic substances, and biological treatment methods feature slow reaction rates and require the disposal of activated sludge.[10,11] Since organic pollutants can be completely degraded into harmless matter by photocatalysis under ambient temperature and pressure, researchers have predicted that it will soon be recognized as one of the most effective means of dealing with various kinds of wastewater.[12]

Bismuth vanadate ($BiVO_4$) is a promising photocatalyst because of its properties such as nontoxicity, high stability, and excellent photocatalytic effect in organic dye degradation.[13–23] It possesses a bandgap of 2.3–2.4 eV, which is smaller than that of the TiO_2 photocatalyst (3.2 eV) and shows good absorption for visible light.[24,25] $BiVO_4$ mainly possesses three crystalline phases[26,27]: monoclinic-scheelite, tetragonal-zircon, and tetragonal-scheelite. Among the three crystalline phases, the monoclinic-scheelite structure shows the best photocatalytic activity under visible-light irradiation because of its narrower band gap (2.4 eV)[28] than that of tetragonal structure (2.9 eV).[29]

To the best of our knowledge, no prior study has investigated the degradation of pirimicarb insecticides using a bi-based photocatalyst, and very little is known about the use of $BiVO_4$ in the treatment of pirimicarb in aqueous solutions. This paper first addresses the optimization of $BiVO_4$-mediated photocatalytic degradation of pirimicarb through a systematic investigation of the effect of different operational variables such as hydrogen peroxide concentration, catalyst dosage, solution pH, and the

CONTACT Chungshin Lu cslu6@nutc.edu.tw Department of General Education, National Taichung University of Science and Technology, Taichung 404, Taiwan, Republic of China.

Color versions of one or more of the figures in the article can be found online at www.tandfonline.com/lsst.

presence of anions. It then provides a better understanding of the contribution of some major reactive species (HO•, h^+, $•O_2^-$) in the photocatalytic process by the addition of the scavengers isopropanol, EDTA, and methanol. Third, this study seeks to identify the reaction intermediates and understand the mechanistic details of the photodegradation of pirimicarb in the $BiVO_4$/visible-light process. Finally, the practicality of this $BiVO_4$ photocatalyst is validated for the degradation of pirimicarb in environmental water samples (river water and lake water).

Experimental

Materials

Pirimicarb insecticide (Sigma, St. Louis, MO, USA), $Bi(NO_3)_3·5H_2O$ (Sigma), NH_4VO_3 (Panreac, Barcelona, Spain), isopropanol (Merck, Kenilworth, NJ, USA), ethylene diamine tetraacetic acid (Alfa Aesar, Lancashire, UK), and methanol (Merck) were obtained and used without any further purification. A stock solution containing 10 mg L^{-1} of pirimicarb in water was prepared, protected from light, and stored at 4°C. HPLC analysis was used to confirm the presence of pirimicarb as a pure organic compound. Hydrogen peroxide (30%) was purchased from Acros Organics (Geel, Belgium) and all other chemicals were of reagent grade and used as such without further purification. Deionized water was used throughout this study. The water was purified with a Milli-Q water ion-exchange system (Millipore Co., Billerica, MA, USA) for a resistivity of 1.8×10^7 Ω-cm.

Preparation and characterization of $BiVO_4$

A quantity of 19.4 g of $Bi(NO_3)_3·5H_2O$ and 4.679 g of NH_4VO_3 were separately added into two solutions of 2.0 mol L^{-1} nitric acid (500 mL) with stirring over 30 min at room temperature. After the solutions of $Bi(NO_3)_3·5H_2O$ and NH_4VO_3 mixed with each other, 7.5 g of urea was added. Then the mixed solution was refluxed and stirred for 24 h at 90°C. The vivid yellow precipitate was washed several times with distilled water and absolute alcohol, and then dried at 60°C for 10 h. Finally, the dried powder was calcined at 450°C for 15 min.

The phase and composition of the as-prepared $BiVO_4$ powder were measured using an X-ray diffractometer (PHILIPS X'PERT Pro MPD, Almelo, Netherlands). The morphology of $BiVO_4$ powder was analyzed using a field-emission scanning electron microscope (FE-SEM, HITACHI S-4800, Krefeld, Germany). The UV–vis diffuse reflectance spectrum of the $BiVO_4$ powder was measured using a UV–vis spectrophotometer equipped with an integration sphere (Perkin Elmer Lambda 35, Waltham, MA, USA). The Brunauer–Emmett–Teller (BET) surface area of the $BiVO_4$ powder was analyzed by nitrogen adsorption–desorption measurement (ASAP 2020, Norcross, USA).

Apparatus and instruments

The apparatus used to study the photocatalytic degradation of pirimicarb is described elsewhere.[30] The C-75 Chromato-Vue UVP cabinet provided a wide area of illumination from 4 W visible-light tubes positioned on two sides of the cabinet interior. A Waters ZQ LC/MS system, equipped with a binary pump, a photodiode array detector, an autosampler, and a micromass detector, was used for separation and identification.

Procedures and analysis

Degradations were performed on 100 mL of aqueous solutions containing 10 mg L^{-1} pirimicarb and four different amounts of $BiVO_4$ (0.1, 0.25, 0.5, and 1.0 g L^{-1}) at different pH values. For reactions in different pH media, the initial pH of the suspension was adjusted by adding either NaOH or HNO_3 solution. Prior to irradiation, the suspension was magnetically stirred in the dark for ca. 30 min to ensure the establishment of an adsorption–desorption equilibrium. Different amounts of hydrogen peroxide (0.35, 1.05, or 1.75 g L^{-1}) were then added. Irradiation was carried out using two fluorescent lamps (F4T5/CW, Philips Lighting Co., Salina, KS, USA). The lamp mainly provides visible light in the range of 400–700 nm. The average light intensity striking the surface of the reaction solution was about 1420 lux, as measured by a digital luxmeter. At any given irradiation time interval, the suspension was sampled (5 mL) and centrifuged to separate the $BiVO_4$ powders.

After each irradiation cycle, the amount of the pirimicarb residual was determined by HPLC. The analysis of organic intermediates was accomplished by HPLC-ESI-MS after readjustment of chromatographic conditions to make the mobile phase compatible with the working conditions of the mass spectrometer. Solvent A was 25 mM aqueous ammonium acetate buffer (pH 6.9), and solvent B was methanol. LC was carried out on an Atlantis™ dC18 column (250 mm × 4.6 mm i.d., d_p = 5 μm). The flow rate of the mobile phase was set at 1 mL min^{-1}. A linear gradient was run as follows: $t = 0$, $A = 95$, $B = 5$; $t = 20$, $A = 50$, $B = 50$; $t = 35$–40, $A = 10$, $B = 90$; and, $t = 45$, $A = 95$, $B = 5$. The elution was monitored at 220 nm. The column effluent was introduced into the ESI source of the mass spectrometer. The quadruple mass spectrometer, equipped with an ESI interface with a heated nebulizer probe at 350°C, was used

with an ion source temperature of 80°C. ESI was carried out with the vaporizer at 350°C, and nitrogen was used as sheath (80 psi) and auxiliary (20 psi) gas to assist with the preliminary nebulization and to initiate the ionization process. A discharge current of 5 μA was applied. Tube lens and capillary voltages were optimized for maximum response during the perfusion of the pirimicarb standard.

Analysis of hydroxyl radicals

The formation of hydroxyl radicals (HO•) in the Vis/$BiVO_4$/H_2O_2 system was detected by the fluorescence technique using coumarin as a probe molecule. The experimental procedures were similar to those used in the measurement of photocatalytic activity except that the aqueous solution of pirimicarb was replaced by an aqueous solution of 1×10^{-3} M coumarin. Visible-light irradiation was continuous and sampling was performed every 2 h for analysis. The solution was analyzed after filtration on a Shimadzu RF-5301PC fluorescence spectrophotometer. The product of the coumarin hydroxylation, 7-hydroxycoumarin, produced a peak at a wavelength of about 456 nm by excitation with a wavelength of 332 nm.

Procedure for degradation of pirimicarb in real samples

The river water sample was collected from the Han River in Taichung city, while the lake water sample was collected from the lake in Taichung Park. Real water samples were collected in Pyrex borosilicate glass or PET containers. Once transported to the lab, all samples were filtered through 0.45 μm membranes to remove suspended matter and stored in the dark at 4°C until analysis. Finally, the real water samples were spiked with the target compound (at 10 mg L^{-1}) just prior to photocatalytic experiments. Degradations were performed on 100 mL of real water samples containing 0.5 g L^{-1} $BiVO_4$ and 1.05 g L^{-1} H_2O_2 at pH 5.

Results and discussion

Characterization of $BiVO_4$

Figure 1 shows the XRD pattern, SEM image, and DRS analysis of the as-prepared $BiVO_4$ photocatalyst. The $BiVO_4$ photocatalyst has a monoclinic-scheelite structure and the diffraction peaks of the sample conform with the standard $BiVO_4$ (JCPDS 14-0688) with a = 5.195 Å, b = 11.701 Å, and c = 5.092 Å. The sharp and narrow diffraction peaks indicate a high crystallinity of the monoclinic $BiVO_4$. No diffraction peaks of other phases are detected. SEM analysis indicates that the microparticles of the $BiVO_4$ sample are mainly polyhedral in morphology (6–8 μm in edge length). The BET surface area of $BiVO_4$ was determined to be 0.40 m^2/g. According to the diffuse reflectance spectrum, the $BiVO_4$ powder presents photoabsorption properties from the UV-light region to visible-light region until 550 nm. The band gap (E_g) of $BiVO_4$ is estimated to be 2.35 eV, which indicates that the $BiVO_4$ sample has a band gap suitable for the photocatalytic decomposition of organic contaminants under visible-light irradiation.[31]

The XPS spectra of the as-prepared $BiVO_4$ exhibited the characteristic spin–orbit split of Bi4f 5/2 and Bi4f 7/2 signals, V2p 1/2 and V2p 3/2 signals, and O1s peak (Fig. 2). The Bi4f orbital showed splitting peaks at 158.9 and 164.2 eV, and the V2p orbital showed the peaks at 516.8 and 524.2 eV. The observed O1s peak at 530.2 eV could be assigned to the lattice oxygen in crystalline $BiVO_4$.[32]

Effect of H_2O_2 dosage

To investigate the effect of adding H_2O_2 to the photocatalysis of pirimicarb, experiments with the as-prepared $BiVO_4$ and different dosages of H_2O_2 were carried out under visible-light irradiation. The results indicate that, if only the $BiVO_4$ powder is added to the solution under visible-light irradiation, pirimicarb did not show photodegradation (Fig. 3). However, the degradation rate can be significantly increased by adding H_2O_2 to the process. This might be due to the difficult migration of photoinduced carriers within the pure $BiVO_4$ catalyst[33]; hence, without proper scavengers for photogenerated carriers, electrons and holes could easily recombine, thus reducing photocatalytic efficiency. Here, radical precursor H_2O_2 may induce the generation of oxidizing species (HO•) and simultaneously act as electron acceptor to prevent the recombination of electron and hole, thus contributing to the photocatalytic oxidation of organic contaminants.[34] The HO• generated had a strong oxidizing ability and was available to oxidize pirimicarb. Therefore, the appropriate amount of additive H_2O_2 could enhance the photocatalytic degradation efficiency.

Nevertheless, there is an optimum dosage for H_2O_2; too high or too low dosage could decrease the degradation efficiency. The highest degradation efficiency was observed in the system with 1.05 g L^{-1} H_2O_2, which could degrade 99.8% of pirimicarb in 8 h. As shown in Fig. 3, insufficient H_2O_2 results in insufficient amounts of HO• being generated to act as an oxidizer, thus reducing photocatalytic activity. At high H_2O_2 dosages, however, the excess H_2O_2 molecules scavenged the valuable HO• and generated a much weaker oxidant HO_2•, which could further react

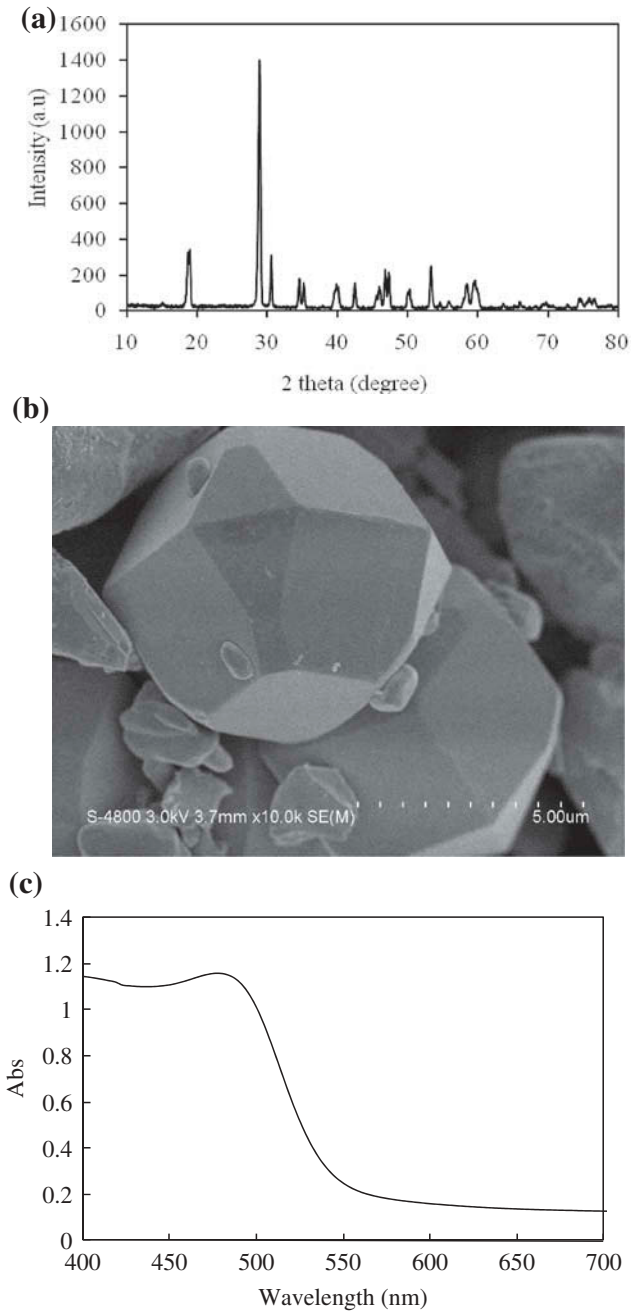

Figure. 1. (a) XRD pattern, (b) SEM image, and (c) DRS analysis of the as-prepared $BiVO_4$ photocatalyst.

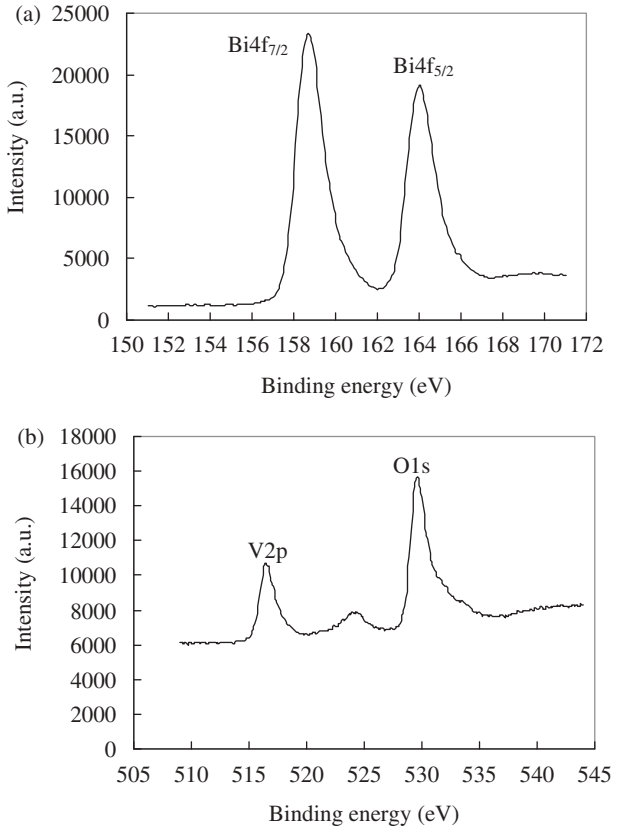

Figure. 2. XPS spectra of the as-prepared $BiVO_4$ photocatalyst: (a) Bi4f; (b) V2p and O1s.

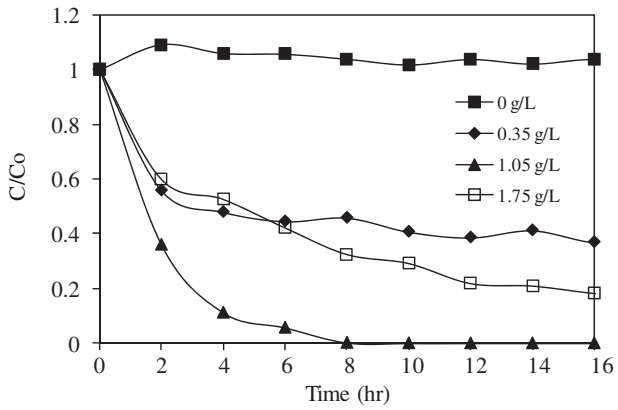

Figure 3. Effect of H_2O_2 dosage on the photocatalytic degradation rate of pirimicarb. Experimental conditions: pirimicarb concentration, 10 mg L^{-1}; $BiVO_4$ concentration, 1 g L^{-1}; pH 5.

with the remaining strong HO• to form oxygen and water.[35] Therefore, the total oxidation capabilities of the system are largely reduced and the rates retarded.

Effect of catalyst dosage

To obtain the optimum $BiVO_4$ suspension concentration, the effect of photocatalyst dosages on the degradation of pirimicarb in aqueous solution was studied, and experiments were carried out using $BiVO_4$ concentrations ranging from 0.1 to 1.0 g/L. The results showed that the photocatalytic reaction without $BiVO_4$ produced the lowest activity (Fig. 4). As the concentration of the photocatalyst increases from 0.1 to 0.5 g/L, the photodegradation efficiency of pirimicarb increases rapidly from 67.7% to 92.4% under visible-light irradiation for 3 h. The efficiency then decreases slightly when the $BiVO_4$ concentration exceeds 0.5 g/L. Below the optimal catalyst loading, dosing more catalyst to the reaction solution

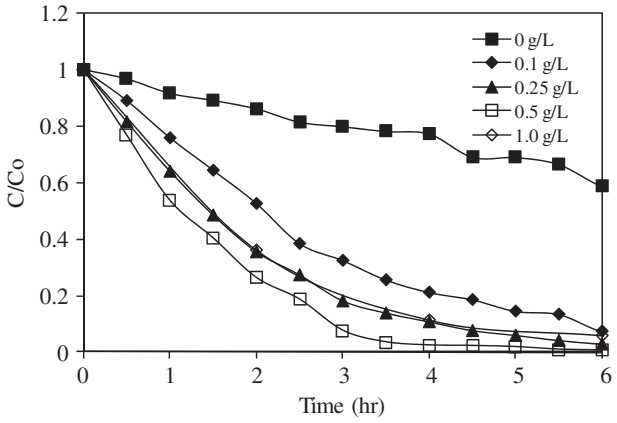

Figure 4. Effect of $BiVO_4$ dosage on the photocatalytic degradation rate of pirimicarb. Experimental conditions: pirimicarb concentration, 10 mg L^{-1}; H_2O_2 concentration, 1.05 g L^{-1}; pH 5.

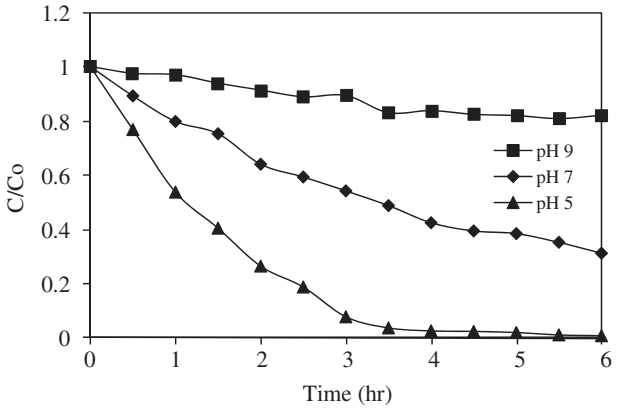

Figure 5. pH effect on the photocatalytic degradation rate of pirimicarb. Experimental conditions: pirimicarb concentration, 10 mg L^{-1}; $BiVO_4$ concentration, 0.5 g L^{-1}; H_2O_2 concentration, 1.05 g L^{-1}.

results in a higher initial degradation rate. This may be attributed to the higher amount of total active surface area, that is, a larger number of active surface sites and a more pronounced light absorption when the added catalyst mass increases.[36] Above the optimal catalyst loading, the initial degradation rate decreases with higher catalyst concentrations. The excessive $BiVO_4$ photocatalyst increases turbidity and opacity of the solution with scattering phenomena reducing the light transmission through the solution (shielding effect).[37] At high catalyst concentrations, particle aggregation may also reduce the catalytic activity,[38] thus decreasing photodegradation efficiency of pirimicarb.

Effect of initial pH value

Many studies have indicated that the pH of a solution is an important parameter in the photocatalytic degradation of organic compounds.[39,40] Figure 5 shows the influence of the initial pH value on the photodegradation rate of pirimicarb in the Vis/$BiVO_4$/H_2O_2 system. The results indicate that the degradation rate decreased as pH increased, and this degradation proceeded much faster under an acidic pH. When the initial pH rose from 5.0 to 9.0, the degradation rate of pirimicarb within 3 h decreased significantly from 92.4% to 10.7%. At higher pH levels, the reduced photocatalytic performance of $BiVO_4$/H_2O_2 under visible-light irradiation was likely due to a special property of H_2O_2[41] in that, in an alkaline medium, H_2O_2 becomes highly unstable resulting in the self-decomposition of H_2O_2, and this phenomenon is strongly dependent on pH.[42] The self-decomposition would rapidly break down the H_2O_2 molecules into water and oxygen, and results in the molecule losing its oxidizing characteristics and, most importantly, no longer serving as a source of hydroxyl radicals. The degradation rate of pirimicarb in the Vis/$BiVO_4$/H_2O_2 process was therefore significantly reduced at higher pH values.

Effects of anions

To investigate the effect of inorganic anions that are most likely to be found in natural waters, NaCl, $NaNO_3$, and Na_2SO_4 were added to the system until the resultant solution contained 0.05 M of Cl^-, NO_3^-, and SO_4^{2-} ions prior to irradiation. The results showed that all these anions significantly inhibited the degradation (see Fig. 6). The inhibition effects of anions could be explained as the reaction of positive holes (h^+) and hydroxyl radical (HO•) with anions that behaved as h^+ and HO• scavengers resulting in prolonged pirimicarb removal.[43] A major drawback resulting from the high reactivity and nonselectivity of HO• was that it also reacted with nontarget compounds present in the background water matrix, that is, inorganic anions present in water. Thus, a greater quantity of HO• was needed to achieve the desired degree of degradation.[44]

Detection of active species by scavengers

To evaluate the role of the active species involved in the photocatalytic process, isopropanol (IPA), ethylenediamine tetraacetic acid (EDTA), and methanol (MeOH) were respectively added as active species scavengers for HO•, h^+, and $\bullet O_2^{-\cdot}$.[45] Figure 7 displays the photocatalytic degradation of pirimicarb with the $BiVO_4$ catalyst in the absence and presence of scavengers (IPA, EDTA, and MeOH) under visible-light irradiation. It can be observed that the addition of MeOH induces a small change in the degradation efficiencies of pirimicarb, which suggests that $\bullet O_2^-$ radicals do not play a major

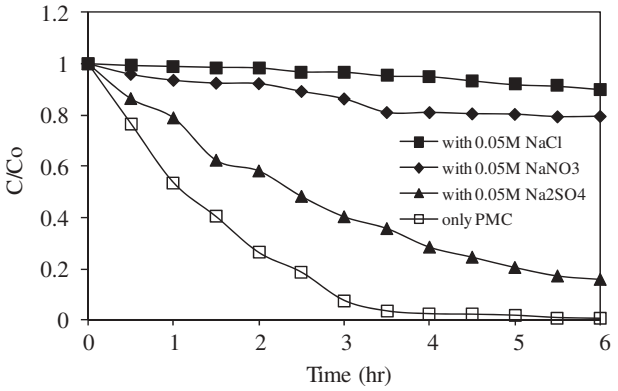

Figure 6. Effect of anions on the photocatalytic degradation rate of pirimicarb. Experimental conditions: pirimicarb concentration, 10 mg L^{-1}; $BiVO_4$ concentration, 0.5 g L^{-1}; H_2O_2 concentration, 1.05 g L^{-1}; pH 5.

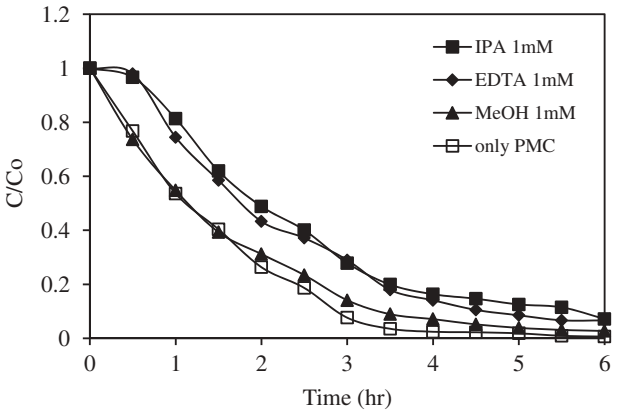

Figure 7. Photocatalytic degradation of pirimicarb with $BiVO_4$ catalyst in the absence and presence of scavengers (IPA, EDTA, and MeOH) under visible-light irradiation. Experimental conditions: pirimicarb concentration, 10 mg L^{-1}; scavenger concentration, 1×10^{-3} M; $BiVO_4$ concentration, 0.5 g L^{-1}; H_2O_2 concentration, 1.05 g L^{-1}; pH 5.

role for the photocatalytic degradation of pirimicarb. On the contrary, IPA and EDTA have obvious inhibition on the photocatalytic degradation of pirimicarb, which suggests that hydroxyl radicals and photogenerated holes are the dominant oxidative species in the photocatalytic system.

We further confirmed the formation of hydroxyl radical by the fluorescence technique using coumarin as a probe molecule. When HO• radicals are formed they react with coumarin to form 7-hydroxycoumarin, which shows a fluorescence peak at 456 nm under an excitation wavelength of 332 nm.[46] Figure 8shows the changes of fluorescence spectra from 10^{-3} M coumarin solution under visible-light irradiation with irradiation time in the presence of $BiVO_4/H_2O_2$. A gradual increase in the fluorescence intensity at about 456 nm was observed with

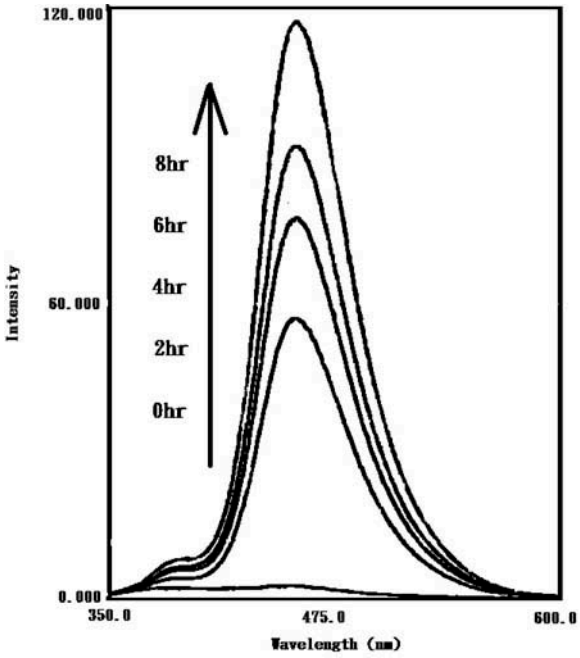

Figure 8. Fluorescence spectral changes observed during illumination of $BiVO_4/H_2O_2$ in a 1×10^{-3} M aqueous solution of coumarin (excitation at 332 nm). Each fluorescence spectrum was recorded every 2 h of visible-light irradiation.

increasing irradiation time. The generated fluorescence spectrum had an identical shape and maximum wavelength to that of standard 7-hydroxycoumarin. This suggested that fluorescent product 7-hydroxycoumarin was formed during $BiVO_4$ photocatalysis due to the specific reaction between HO• and coumarin. Therefore, hydroxyl radicals were shown to be the active species during $BiVO_4$ photocatalytic reaction.

From Fig. 3, we can observe that if only the $BiVO_4$ powder is added to the solution under visible-light irradiation, pirimicarb did not show photodegradation because the photogenerated carriers (electrons and holes) could easily recombine. However, if $BiVO_4/H_2O_2$ is added to the solution during irradiation, hydroxyl radicals can be formed in significant amount (Fig. 8) and the degradation rate can be significantly increased. These results are in agreement with Xiang *et al.*[46] and Saison *et al.*[47].

Separation and identification of the intermediates

Considering the environmental concerns regarding pirimicarb and the limited data in the literature with regard to the reaction intermediates generated during the removal of this pollutant, a thorough product study on the degradation of pirimicarb in dilute aqueous solution using the Vis/$BiVO_4/H_2O_2$ process was undertaken. Figure 9 shows a total ion chromatogram of the

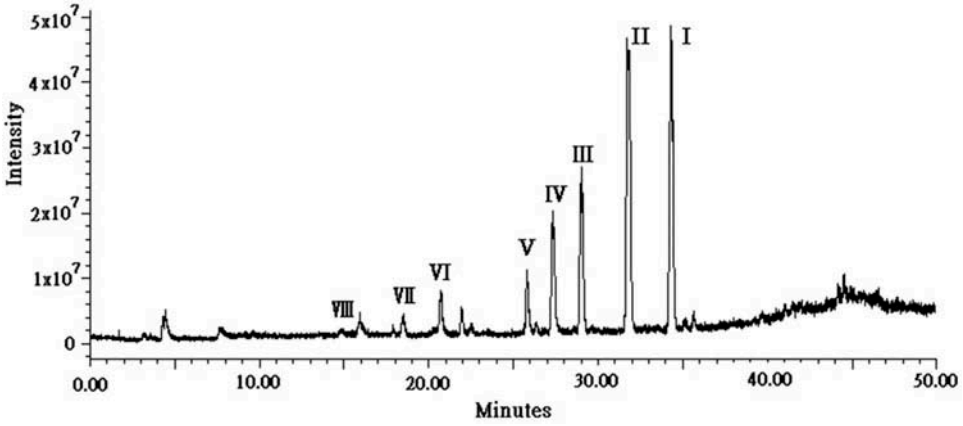

Figure 9. Total ion chromatogram obtained for pirimicarb solution (100 mg L^{-1}) after 9 h of irradiation with visible light in the presence of $BiVO_4$ (0.5 g L^{-1}) and H_2O_2 (1.05 g L^{-1}).

pirimicarb solution in the presence of both H_2O_2 and $BiVO_4$ catalyst under visible-light irradiation. The solution contained at least eight identified components at retention times of less than 50 min. One of the peaks was the initial pirimicarb (peak I); the other seven (new) peaks were those of the intermediates formed. We denote the pirimicarb and its related intermediates as compounds I–VIII. Except for the initial pirimicarb, the other peaks increased at first and subsequently decreased, indicating the formation and subsequent transformation of the intermediates.

Table 1 presents the retention times and mass peaks of the intermediates and the corresponding compounds identified by interpretation of their mass spectra. Compound II was identified as 2-[(methylformyl)amino]-5,6-dimethylpyrimidin-4-yl-dimethylcarbamate and exhibited a protonated molecular ion peak at $m/z = 253$ and a fragment ion at $m/z = 225$, which corresponded to the $[M \pm H–CH_2–CH_2]^{\pm}$ group. The mass spectra data showed that the *N*-methyl group of pirimicarb had been oxidized and transformed into an aldehyde group.[1] Compound III was identified as 2-methylamino-5,6-dimethylpyrimidin-4-yl-dimethylcarbamate and exhibited a protonated molecular ion peak at $m/z = 225$, which corresponded to the loss of one methyl group from pirimicarb. It exhibited a fragment ion at $m/z = 168$ which corresponded to the $[M \pm H–NCH_3–CH_2–CH_2]^{\pm}$ group. This compound was probably produced by the demethylation of the 2-dimethylamino group of pirimicarb.

Table 1. Identification of the intermediates from the photodegradation of pirimicarb by HPLC-ESI-MS.

Peaks	Photodegradation intermediates	Abbreviation	RT (min)	MS peaks (*m/z*)
I	2-dimethylamino-5,6-dimethylpyrimidin-4-yl-dimethylcarbamate	DDP	34.33	239
II	2-[(methylformyl)amino]-5,6-dimethylpyrimidin-4-yl-dimethylcarbamate	MFDP	31.81	253, 225
III	2-methylamino-5,6-dimethylpyrimidin-4-yl-dimethylcarbamate	MDP	29.05	225, 168
IV	2-(formylamino)-5,6-dimethylpyrimidin-4-yl-dimethylcarbamate	FDP	27.32	239, 211
V	2-amino-5,6-dimethylpyrimidin-4-yl-dimethylcarbamate	ADP	25.81	211, 154
VI	2-dimethylamino-5,6-dimethyl-4-hydroxypyrimidine	DDHP	20.69	168
VII	2-methylamino-5,6-dimethyl-4-hydroxypyrimidine	MDHP	18.49	154
VIII	2-amino-5,6-dimethyl-4-hydroxypyrimidine	ADHP	14.84	140

Compound IV was identified as 2-(formylamino)-5,6-dimethylpyrimidin-4-yl-dimethylcarbamate and exhibited a protonated molecular ion peak at $m/z = 239$ and a fragment ion at $m/z = 211$, which corresponded to the $[M \pm H–CH_2–CH_2]^{\pm}$ group. This compound was produced by the oxidation of the *N*-methyl group of compound III. Compound V was identified as 2-amino-5,6-dimethylpyrimidin-4-yl-dimethylcarbamate and exhibited a protonated molecular ion peak at $m/z = 211$, which corresponded to the loss of two methyl groups from pirimicarb. It exhibited a fragment ion at $m/z = 154$, which corresponded to the $[M \pm H–NCH_3–CH_2–CH_2]^{\pm}$ group. It was probably produced by the demethylation at the 2-methylamino group of compound III.

Compound VI was identified as 2-dimethylamino-5,6-dimethyl-4-hydroxypyrimidine and exhibited a protonated molecular ion peak at $m/z = 168$. This compound was produced by the alpha-cleavage of the carbonyl–oxygen bond and transformed into corresponding phenol.[1] Compounds VII and VIII were, respectively, identified as 2-methylamino-5,6-dimethyl-4-hydroxypyrimidine and 2-amino-5,6-dimethyl-4-hydroxypyrimidine, exhibiting protonated molecular ion peaks at $m/z = 154$ and $m/z =$

140. They were probably produced by the demethylation at the 2-dimethylamino group of DDHP (compound VI).

The absorption spectra of these intermediate products are measured and depicted in Fig. 10. The absorption maximum of the spectral bands shifts hypsochromically from 245.3 nm (Fig. 10a, spectrum I) to 227.6 nm (Fig. 10a, spectrum V), and from 225.2 nm (Fig. 10c, spectrum VI) to 219.3 nm (Fig. 10c, spectrum VIII). These hypsochromic shifts of the absorption bands are presumed to result from the formation of a series of *N*-de-methylated intermediates in a stepwise manner. The *N*-de-methylation of the 2-dimethylamino-5,6-dimethylpyrimidin-4-yldimethylcarbamate (pirimicarb) has the wavelength position of its major absorption band moved toward the blue region, λ_{max}, I, 245.3 nm; III, 237 nm; V, 227.6 nm. Moreover, in Fig. 10c, the hypsochromic shift of the absorption band presumably results from the formation of a series of hydroxypyrimidine derivatives in a stepwise manner. The *N*-de-methylation of the 2-dimethylamino-5,6-dimethyl-4-hydroxypyrimidine has the wavelength position of its major absorption band moved toward the blue region, λ_{max}, VI, 225.2 nm; VII, 221.7 nm; VIII, 219.3 nm.

Degradation pathways of pirimicarb

Based on the results, the molecular structure of the degradation intermediates and the tentative photocatalytic degradation pathway of pirimicarb are presented

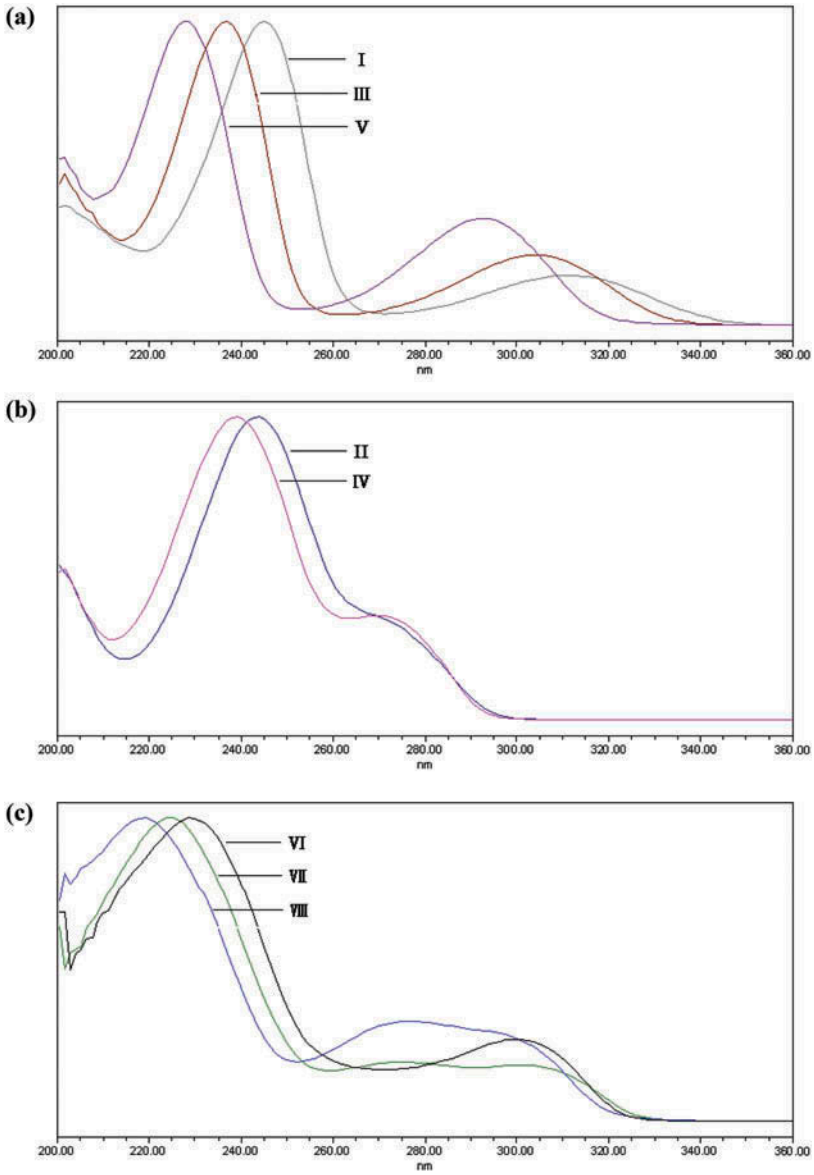

Figure 10. Absorption spectra of the intermediates formed during the photodegradation of pirimicarb. Spectra were recorded using the photodiode array detector. (a) Spectra I, III, V; (b) spectra II, IV; and (c) spectra VI–VII correspond to the peaks I, III, V, II, IV, and VI–VIII in Fig. 9, respectively.

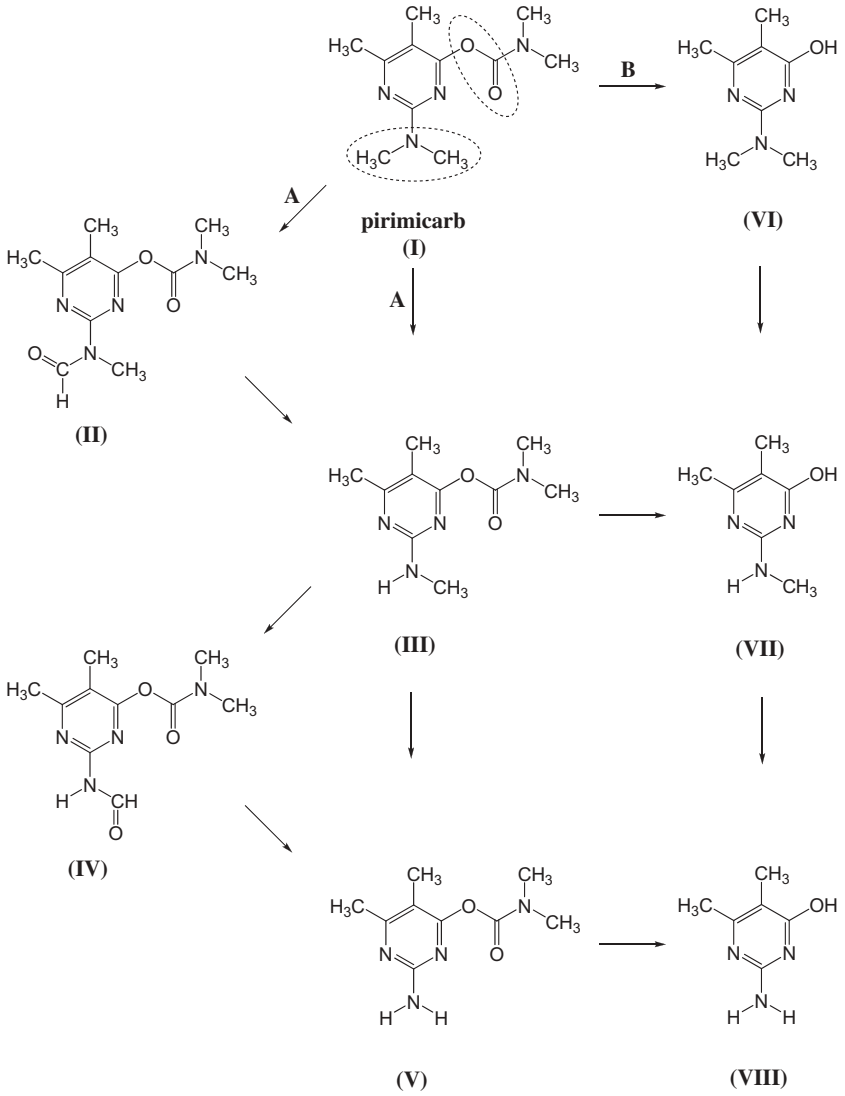

Figure 11. Proposed photocatalytic degradation mechanism of pirimicarb followed by the identification of several intermediates by HPLC-ESI-MS technique.

in Fig. 11. It involves two different pathways (routes A and B, respectively), corresponding to the two possible reaction sites on the pirimicarb molecule. One was based on successive *N*-dealkylation of the 2-dimethylamino group to form the carbamate-containing intermediates II–V. The second degradation route was based on decarbamoylation of the carbamate moiety with further *N*-dealkylation of the 2-dimethylamino group to have the hydroxypyrimidines VI–VIII.

The *N*-dealkylation of the pirimicarb occurs mostly due to the attack of the HO• species on the 2-dimethylamino group of the pirimicarb. It is well known that the HO• radical is an electrophile and that C–H bonds adjacent to nitrogen are responsible for a pronounced stereoelectronic effect that produces high rates of H-atom abstraction. Therefore, the hydrogen atoms in the 2-dimethylamino group of pirimicarb molecule are the most prone to radical attack. Hydroxyl radicals yielded carbon-centred radicals upon the H-atom abstraction from the *N*-methyl group, or they reacted with the lone-pair electron on the N atom to generate cationic radicals, which are subsequently converted into carbon-centred radicals.[48] The carbon-centred radical generated following the addition of oxygen forming the peroxyl radical decomposed to different intermediates (compounds II and III). The mono-de-methylated species (compound III) can also be degraded by $BiVO_4$ photocatalysis and is implicated in other similar events (H-atom abstraction and oxygen attack) to yield the corresponding *N*-formyl intermediate (compound IV) and bi-de-methylated intermediate (compound V).

In the second route, pirimicarb (I) was subjected to chemical decarbamoylation to produce 2-dimethylamino-5,6-dimethyl-4-hydroxypyrimidine (compound

VI). The degradation pathway was via the cleavage of the carbonyl–oxygen bond to give the corresponding hydroxypyrimidine. Decarbamoylation of the carbamate moiety of compound III or *N*-dealkylation of the 2-dimethylamino group of compound VI would then yield 2-methylamino-5,6-dimethyl-4-hydroxypyrimidine (compound VII). Further *N*-dealkylation of compound VII or decarbamoylation of the carbamate moiety of compound V induced the formation of 2-amino-5,6-dimethyl-4-hydroxypyrimidine (compound VIII).

Performance of recycled catalyst

To confirm the stability of the high photocatalytic performance of $BiVO_4$, the circulating runs in the photocatalytic degradation of pirimicarb in Vis/$BiVO_4$/H_2O_2 system was performed (Fig. 12). After five recycles for the photodegradation of pirimicarb, the catalyst did not exhibit any significant loss of activity. It indicates that $BiVO_4$ has high stability and does not photocorrode during the photocatalytic oxidation of pirimicarb, which is especially important for its application.

Treatment of real water samples

To evaluate whether the $BiVO_4$ photocatalysis system can be applied to environmental water, we collected lake and river water samples for testing. The degradation rates of pirimicarb in deionized water and real water samples are compared in Fig. 13. For the environmental water samples, the pirimicarb concentration in Vis/$BiVO_4$/H_2O_2 process decreased with an increase in the irradiation time, indicating that the as-prepared material is an active photocatalyst. The degradation rate of pirimicarb using $BiVO_4$ photocatalytic system in river water was slightly decreased in comparison with that in deionized water. This result may be due to the fact that anions or hydroxyl radical scavengers in the river water samples decreased the photocatalytic activity of $BiVO_4$. From Fig. 6, we can observe an inhibitive effect of anions in the order $SO_4^{-2} < NO_3^- < Cl^-$ during the photocatalytic degradation of pirimicarb. Considering the characteristics of the real water sample given in Table 2, the presence of inorganic anions such as chloride and nitrate in the composition of river water could hinder the oxidation process by scavenging the produced hydroxyl radicals. However, $BiVO_4$ photocatalysis can be used for effective degradation of pirimicarb in real water samples, indicating its potential for practical applications in water pollutant removal and environmental remediation.

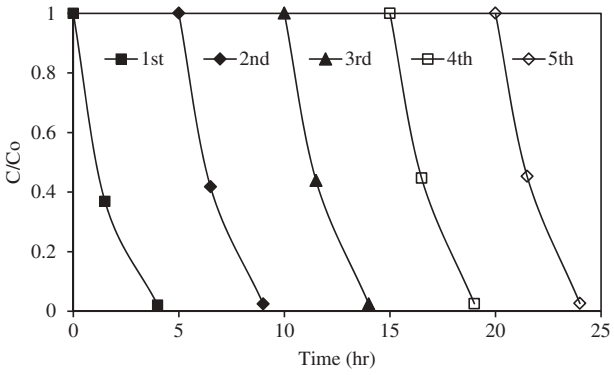

Figure 12. Cycling runs in the photocatalytic degradation of pirimicarb in the presence of $BiVO_4$/H_2O_2 under visible-light irradiation. Experimental conditions: pirimicarb concentration, 10 mg L^{-1}; $BiVO_4$ concentration, 0.5 g L^{-1}; H_2O_2 concentration, 1.05 g L^{-1}; pH 5.

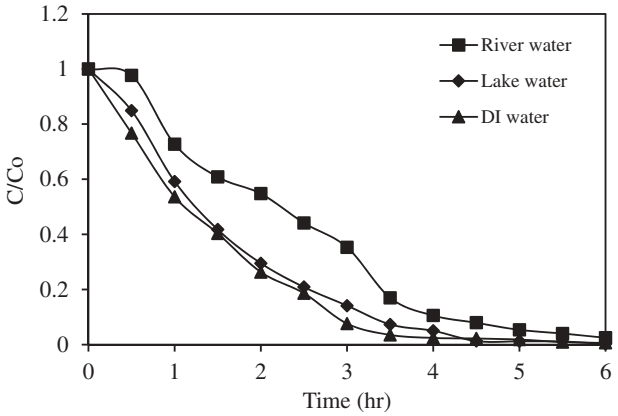

Figure 13. Photocatalytic degradation rates of pirimicarb in deionized and real water samples. Experimental conditions: $BiVO_4$ concentration, 0.5 g L^{-1}; H_2O_2 concentration, 1.05 g L^{-1}; pH 5.

Conclusions

As-prepared $BiVO_4$ powder exhibits the typical pattern of a monoclinic-scheelite structure and shows a high degree of photocatalytic activity under visible-light irradiation. The $BiVO_4$ photocatalysis must be done in the presence of significant amounts of hydrogen peroxide for eliminating pirimicarb insecticides. Four hours of photocatalytic reac-

Table 2. Characteristics of the real water sample.

Parameter	River water	Lake water
pH	6.30	6.24
Conductivity (μmho cm^{-1})	420	378
Turbidity (NTU)	2.9	4.9
Sulfate (mg L^{-1})	48.1	50.9
Chloride (mg L^{-1})	22.6	16.7
Nitrate (mg L^{-1})	84.8	2.9
Nitrite (mg L^{-1})	1.12	0.02

tions reduced pirimicarb concentrations by 97.6%. The photodegradation rate is found to increase with $BiVO_4$ dosage, but the reaction is slower at high dosages. The photodegradation is much more efficient under acidic conditions and decreases with increasing pH. In addition, the presence of inorganic anions such as chloride, nitrate, and sulfate, which are often present in natural water and industrial wastewater, decreases the primicarb photocatalytic degradation rate. The effects of the active species involved in the photocatalytic process are examined. The results indicate that holes and hydroxyl radicals are the main active species involved in the degradation of pirimicarb. Seven intermediates are identified and characterized through a mass spectra analysis, giving insight into the early steps of the degradation process. Based on the identification of intermediates, a simple degradation pathway is tentatively proposed, including *N*-dealkylation of the 2-dimethylamino group and decarbamoylation of the carbamate moiety in the pirimicarb molecule. Finally, the Vis/$BiVO_4$/H_2O_2 process is used for effective degradation of pirimicarb in environmental water samples (river water and lake water), demonstrating the advantages of its high photocatalytic activity.

Funding

This research was supported by the Ministry of Science and Technology of the Republic of China (MOST 103-2113-M-025-001).

References

[1] Chen, T.; Fu, F.; Chen, Z.; Li, D.; Zhang, L.; Chen, G. (2009) Study on the photodegradation and microbiological degradation of pirimicarb insecticide by using liquid chromatography coupled with ion-trap mass spectrometry. *Journal of Chromatography A*, 1216: 3217–3222.

[2] Wang, Y.; Yang, B.; Zhang, P.; Zhang, W.; Liu, C.; Shu, X.; Shu, J. (2012) Heterogeneous reactions of pirimiphos-methyl and pirimicarb with NO_3 radicals. *Journal of Physical Chemistry A*, *116*: 10802–10809.

[3] Fenoll, J.; Garrido, I.; Hellín, P.; Flores, P.; Vela, N.; Navarro, S. (2015) Photocatalytic oxidation of pirimicarb in aqueous slurries containing binary and ternary oxides of zinc and titanium. *Journal of Photochemistry and Photobiology A Chemistry, 298*: 24–32.

[4] Zhou, J.; Ma, C.; Zhou, S.; Ma, P.; Chen, F.; Qi, Y.; Chen, H. (2010) Preparation, evaluation and application of molecularly imprinted solid-phase microextraction monolith for selective extraction of pirimicarb in tomato and pear. *Journal of Chromatography A*, 1217: 7478–7483.

[5] Seitz, F.; Bundschuh, M.; Dabrunz, A.; Bandow, N.; Schaumann, G.E.; Schulz, R. (2012) Titanium dioxide nanoparticles detoxify pirimicarb under UV irradiation at ambient intensities. *Environmental Toxicology and Chemistry*, 31: 518–523.

[6] Soloneski, S.; Larramendy, M.L. (2010) Sister chromatid exchanges and chromosomal aberrations in Chinese hamster ovary (CHO-K1) cells treated with the insecticide pirimicarb. *Journal of Hazardous. Materials*, 174: 410–415.

[7] Tomlin, C.D.S. (Ed.) (2009) The Pesticide Manual, 15th Ed., British Crop Protection Council: Surrey.

[8] Fernández-Ramos, C.; Šatínský, D.; Solich, P. (2014) New method for the determination of carbamate and pyrethroid insecticides in water samples using on-line SPE fused core column chromatography. *Talanta*, 129: 579–585.

[9] Shi, Z.; Hu, J.; Li, Q.; Zhang, S.; Liang, Y.; Zhang, H. (2014) Graphene based solid phase extraction combined with ultra high performance liquid chromatography–tandem mass spectrometry for carbamate pesticides analysis in environmental water samples. *Journal of Chromatography A*, 1355: 219–227.

[10] Wang, K.H.; Hsieh, Y.H.; Chou, M.Y.; Chang, C.Y. (1999) Photocatalytic degradation of 2-chloro and 2-nitrophenol by titanium dioxide suspensions in aqueous solution. *Applied Catalysis B: Environmental*, 21: 1–8.

[11] Pelizzetti, E.; Maurino, V.; Minero, C.; Carlin, V.; Pramauro, E.; Zerbinati, O.; Tosato, M. (1990) Photocatalytic degradation of atrazine and other s-triazine herbicides. *Environmental Science & Technology*, 24: 1559–1565.

[12] Chen, S.; Cao, G. (2005) Study on the photocatalytic reduction of dichromate and photocatalytic oxidation of dichlorvos. *Chemosphere*, 60: 1308–1315.

[13] Li, C.J.; Wang, S.P.; Wang, T.; Wei, Y.J.; Zhang, P.; Gong, J.L. (2014) Monoclinic porous $BiVO_4$ networks decorated by discrete g-C_3N_4 nano-islands with tunable coverage for highly efficient photocatalysis. *Small*, 10:2782.

[14] Hu, Y.; Li, D.Z.; Sun, F.Q.; Wang, H.B.; Weng, Y.Q.; Xiong, W.; Shao, Y. (2015) One-pot template-free synthesis of heterophase $BiVO_4$ microspheres with enhanced photocatalytic activity. *RSC Advances*, 5: 54882–54889.

[15] Gu, S.N.; Li, W.J.; Wang, F.Z.; Wang, S.Y.; Zhou, H.L.; Li, H.D. (2015) Synthesis of buckhorn-like $BiVO_4$ with a shell of CeOx nanodots: Effect of heterojunction structure on the enhancement of photocatalytic activity. *Applied Catalysis B: Environmental*, 170−171:186–194.

[16] Obregón, S.; Colón, G. (2014) Heterostructured Er^{3+} doped $BiVO_4$ with exceptional photocatalytic performance by cooperative electronic and luminescence sensitization mechanism. *Applied Catalysis B: Environmental*, 158–159:242–249.

[17] Lin, X.; Yu, L.; Yan, L.; Li, H.; Yan, Y.; Liu, C.; Zhai, H. (2014) Visible light photocatalytic activity of $BiVO_4$ particles with different morphologies. *Solid State Science*, 32: 61–66.

[18] Madhusudan, P.; Ran, J.; Zhang, J.; Yu, J.; Liu, G. (2011) Novel urea assisted hydrothermal synthesis of hierarchical $BiVO_4$/$Bi_2O_2CO_3$ nanocomposites with enhanced visible-light photocatalytic activity. *Applied Catalysis B Environmental*, 110: 286–295.

[19] Guo, Y.; Yang, X.; Ma, F.; Li, K.; Xu, L.; Yuan, X.; Guo, Y. (2010) Additive-free controllable fabrication of

bismuth vanadates and their photocatalytic activity toward dye degradation. *Applied Surface Science*, *256*: 2215–2222.

[20] Madhusudan, P.; Kumar, M. V.; Ishigaki, T.; Toda, K.; Uematsu, K.; Sato, M. (2013) Hydrothermal synthesis of meso/macroporous $BiVO_4$ hierarchical particles and their photocatalytic degradation properties under visible light irradiation. *Environmental Science and Pollution Research*, 20: 6638–6645.

[21] Zhou, L.; Wang, W.; Zhang, L.; Xu, H.; Zhu, W. (2007) Single-crystalline $BiVO_4$ microtubes with square cross-sections: Microstructure, growth mechanism, and photocatalytic property. *Journal of Physical Chemistry C*, 111: 13659–13664.

[22] Lu, Y.; Shang, H.; Shi, F.; Chao, C.; Zhang, X.; Zhang, B. (2015) Preparation and efficient visible light-induced photocatalytic activity of m-$BiVO_4$ with different morphologies. *Journal of Physics and Chemistry of Solids*, 85: 44–50.

[23] Hojamberdiev, M.; Zhu, G.; Kadirova, Z. C.; Han, J.; Liang, J.; Zhou, J.; Wei, X.; Liu, P. (2015) Morphology-controlled growth of $BiVO_4$ crystals by hydrothermal method assisted with ethylene glycol and ethylenediamine and their photocatalytic activity. *Materials Chemistry and Physics*, 165: 188–195.

[24] Xie, B.; Zhang, H.; Cai, P.; Qiu, R.; Xiong, Y. (2006) Simultaneous photocatalytic reduction of Cr(VI) and oxidation of phenol over monoclinic $BiVO_4$ under visible light irradiation. *Chemosphere*, 63: 956–963.

[25] Madhusudan, P.; Zhang, J.; Cheng, B.; Liu, G. (2013) Photocatalytic degradation of organic dyes with hierarchical $Bi_2O_2CO_3$ microstructures under visible-light. *CrystEngComm*, 15: 231–240.

[26] Dong, S.; Feng, J.; Li, Y.; Hu, L.; Liu, M.; Wang, Y.; Pi, Y.; Sun, J.; Sun, J. (2014) Shape-controlled synthesis of $BiVO_4$ hierarchical structures with unique natural-sunlight-driven photocatalytic activity. *Applied Catalysis B: Environmental*, 152–153:413–424.

[27] Xu, J.; Wang, W.Z.; Wang, J.; Liang, Y.J. (2015) Controlled fabrication and enhanced photocatalystic performance of $BiVO_4$@CeO_2 hollow microspheres for the visible-light-driven degradation of rhodamine B. *Applied Surface Science*, 349: 529–537.

[28] Thalluri, S. M.; Hussain, M. Saracco, G. Barber, J.; Russo, N. (2014) Green-synthesized $BiVO_4$ oriented along {040} facets for visible light-driven ethylene degradation. *Industrial & Engineering Chemistry Research*, 53: 2640–2646.

[29] Fan, H.M.; Jiang, T.F.; Li, H.Y.; Wang, D.J.; Wang, L.L.; Zhai, J.L.; He, D.Q.; Wang, P.; Xie, T.F. (2012) Effect of $BiVO_4$ crystalline phases on the photoinduced carriers behavior and photocatalytic activity. *Journal of Physical Chemistry C*, 116: 2425–2430.

[30] Chen, C.C.; Lu, C.S.; Mai, F.D.; Weng, C.S. (2006) Photooxidative *N*-de-ethylation of anionic triarylmethane dye (sulfan blue) in titanium dioxide dispersions under UV irradiation. *Journal of Hazardous Materials. B*, 137: 1600–1607.

[31] Zhang, Z.; Wang, W.; Shang, M.; Yin, W. (2010) Photocatalytic degradation of rhodamine B and phenol by solution combustion synthesized $BiVO_4$ photocatalyst. *Catalysis Communications*, 11: 982–986.

[32] Ge, L. (2008) Novel Pd/$BiVO_4$ composite photocatalysts for efficient degradation of methyl orange under visible light irradiation. *Materials Chemistry Physics*, 107: 465–470.

[33] Dong, S.; Yu, C.; Li, Y.; Li, Y.; Sun, J.; Geng, X. (2014) Controlled synthesis of T-shaped $BiVO_4$ and enhanced visible light responsive photocatalytic activity. *Journal of Solid State Chemistry*, 211: 176–183.

[34] Chu, W.; Rao, Y.F. (2012) Photocatalytic oxidation of monuron in the suspension of WO_3 under the irradiation of UV-visible light. *Chemosphere*, 86: 1079–1086.

[35] Xiao, Q.; Zhang, J.; Xiao, C.; Tan, X.K. (2008) Photocatalytic degradation of methylene blue over Co_3O_4/Bi_2WO_6 composite under visible light irradiation. *Catalysis Communications*, 9: 1247–1253.

[36] Doorslaer, X.V.; Heynderickx, P.M.; Demeestere, K.; Debevere, K.; Langenhove, H.V.; Dewulf, J. (2012) TiO_2 mediated heterogeneous photocatalytic degradation of moxifloxacin: Operational variables and scavenger study. *Applied Catalysis B: Environmental*, 111–112:150–156.

[37] Yu, J.; Zhang, L.; Cheng, B.; Su, Y. (2007) Hydrothermal preparation and photocatalytic activity of hierarchically sponge-like macro-/mesoporous titania. *Journal of Physical Chemistry C*, 111: 10582–10589.

[38] Liu, W.; Chen, S.; Zhao, W.; Zhang, S. (2009) Titanium dioxide mediated photocatalytic degradation of methamidophos in aqueous phase. *Journal of Hazardous Materials*, 164: 154–160.

[39] Leng, W.; Liu, H.; Cheng, S.; Zhang, J.; Cao, C. (2000) Kinetics of photocatalytic degradation of aniline in water over TiO_2 supported on porous nickel. *Journal of Photochemistry and Photobiology A Chem.*, 131: 125–132.

[40] Wang, K.H.; Hisieh, Y.H.; Wu, C.H.; Chang, C.Y. (2000) The pH and anion effects on the heterogeneous photocatalytic degradation of o-methylbenzoic acid in TiO_2 aqueous suspension. *Chemosphere*, 40: 389–394.

[41] Chu, W.; Choy, W.K.; So, T.Y. (2007) The effect of solution pH and peroxide in the TiO_2-induced photocatalysis of chlorinated aniline. *Journal of Hazardous Materials*, 141: 86–91.

[42] Chan, C.Y.; Tao, S.; Dawson, R.; Wong, P.K. (2004) Treatment of atrazine by integrating photocatalytic and biological processes. *Environmental Pollution*, 131: 45–54.

[43] Mahmoodi, N.M.; Arami, M.; Limaee, N.Y.; Gharanjig, K. (2007) Photocatalytic degradation of agricultural *N*-heterocyclic organic pollutants using immobilized nanoparticles of titania. *Journal of Hazardous Materials*, 145: 65–71.

[44] Konstantinou, I.K.; Albanis, T.A. (2004) TiO_2-assisted photocatalytic degradation of azo dyes in aqueous solution: Kinetic and mechanistic investigations, a review. *Applied Catalysis B Environmental*, 49: 1–14.

[45] Dong. S.; Cui, Y.; Wang, Y.; Li, Y.; Hu, L.; Sun, J.; Sun, J. (2014) Designing three-dimensional acicular sheaf shaped $BiVO_4$/reduced graphene oxide composites for efficient sunlight-driven photocatalytic degradation of dye wastewater. *Chemical Engineering Journal*, 249: 102–110.

[46] Xiang, Q.; Yu, J.; Wong, P.K. (2011) Quantitative characterization of hydroxyl radicals produced by various photocatalysts. *Journal of Colloid Interface Science*, 357:163–167.

[47] Saison, T.; Chemin, N.; Chanéac, C.; Durupthy, O.; Mariey, L.; Maugé, F.; Brezová, V.; Jolivet, J.-P. (2015) New insights into $BiVO_4$ properties as visible light photocatalyst. *Journal of Physical Chemistry C*, 119: 12967–12977.

[48] Lee, J.; Choi, W. (2004) Effect of platinum deposits on TiO_2 on the anoxic photocatalytic degradation pathways of alkylamines in water: Dealkylation and *N*-alkylation. *Environmenal Science and Technology*, 38: 4026–4033.